Numerical Simulation of an Ozone-Based Wet-Chemical Etching

Lena Mohr[a)], Tobias Krick, Martin Zimmer, Andreas Fischer and Anamaria Moldovan

Fraunhofer Institute for Solar Energy Systems ISE, Heidenhofstrasse 2, 79110 Freiburg, Germany

[a)]Corresponding author: lena.mohr@ise.fraunhofer.de

Abstract. In the PV-industry, wet-chemical baths are used for surface structuring, conditioning and cleaning. Besides cleaning the wafers, ozone-based wet-chemical cleaning processes show the ancillary effect of intendedly etching back the emitter and/or rounding of textured surfaces. To simulate and predict this rounding of micro-pyramids during the cleaning process, a two dimensional process simulation model was built. With the finite element method of COMSOL Multiphysics the diffusion and convection based mass transport of ozone along the pyramids is described. Important parameters for the evaluation, obtained from experimental results, are the etch rate and resulting roundness (R) of the micro-pyramids tips. A parametric study was carried out with the purpose of adjusting the model. The simulation represents the experimental data accurately, e.g. after 2 min exposure time R = 67 nm for the experimental and R = 66 nm for the simulation data.

INTRODUCTION

Silicon solar cells are produced using a series of different process steps in which wet-chemical etching and rinsing steps have a considerable influence on the quality of the wafers [1]. Etching baths are used for texturing, cleaning and conditioning [2,3]. One widely used approach for wafer cleaning and conditioning is based on dissolved ozone (O_3) in de-ionized water (DI-H_2O) with addition of hydrofluoric acid (HF) and hydrochloric acid (HCl) [3–5]. This approach is especially suited for the production of high efficient solar cells with the ancillary effect of intendedly etching back the emitter e.g. for Passivated Emitter and Rear cells (PERC) [6,7] and rounding of the textured surfaces for Silicon Heterojunction (SHJ) cells [8,9]. The considered process consists of the oxidation of silicon by O_3,

$$\mathrm{Si}+2\mathrm{O}_3\rightarrow\mathrm{SiO}_2+2\mathrm{O}_2 \tag{1}$$

followed by dissolving of the resulting oxide by HF.

$$\mathrm{SiO}_2+6\mathrm{HF}\rightarrow\mathrm{H}_2\mathrm{SiF}_6+2\ \mathrm{H}_2\mathrm{O} \tag{2}$$

It is assumed that (1) is the reaction-rate-determining step, due to the low O_3 concentration (30 mg/l) compared to HF (5 g/l). HCl is added to solvate the metallic and ionic contaminations, [4,10] and maintain them in solution. Besides cleaning, the etching process has a rounding effect on the textured wafer surface [5]. To get a better understanding of this etching reaction, a simulation model according to experimental data was developed representing the rounding effect of the etching solution on the wafer surface. The model is based on the finite element method of COMSOL Multiphysics. The aim is to predict the rounding and etching rates on the entire wafer surface as a function of different process parameters in order to represent and homogenize the flow profiles on the wafer surface.

APPROACH

In order to reduce the simulation complexity, a small area of the entire etching bath was simulated, Fig. 1. During cleaning the solution flows with a volume flow of 40 l/min through the gap (4 mm) between the wafers, along the wafer surface of 100 wafers in a carrier. The parabolic velocity profile of a laminar pipe flow is similar to the laminar velocity profile in rectangular channels with a small aspect ratio (w/h) [11]. Since a laminar flow between the wafers was assumed, the velocity (3) in a small section between two wafers, can be calculated with the analytical velocity profile in a tube for laminar flow [12],

$$v = 2 \cdot v_{av} \left[1 - \left(\frac{2 \cdot s}{w} \right)^2 \right] \tag{3}$$

with v as component of velocity in m/s at the position s, v_{av} as average velocity in m/s, and w as the width of the duct. A section of 0.025 mm was considered instead of the entire 4 mm to minimize the scale between the gap and the pyramid height.

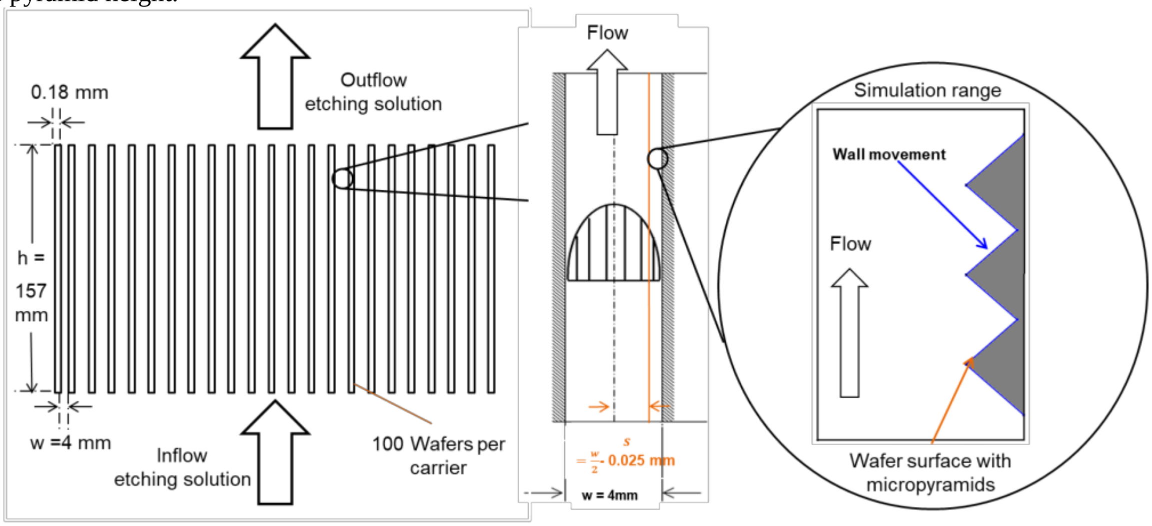

FIGURE 1. Scheme of wafers and flow of the etching solution along the wafer surface, with the simulation range and the 2D simulation model.

The microscopic model represents three pyramids with the acidic solution flowing with a fully developed flow velocity v_y and an ozone start concentration of $c_{O3,0}$ = 15-40 mg/l along the wafer surface. The temperature was kept constant at 30°C. A linear flow was assumed, since v_{av} is 3.4 mm/s and according to Eq.3, v is even slower with a rate of 0.169 mm/s. The cleaning process was described by the etch rate per time (R_{etch}) and roundness (R) of the micro-pyramids tips. R_{etch} was indirectly obtained by the proportionality of the etching removal of the wafer surfaces sheet resistance. With ongoing etching of the emitter, the sheet resistance increased. In [3] an ozone concentration of 15, 30 and 40 mg/l resulted in an etching rate R_{etch} of 5, 9 and 11 nm/min, respectively. In a previous work, R could be determined from the radius of curvature, Fig. 2. R is defined as the radius of an imaginative circle, fitting exactly the pyramid tip of a two dimensional image determined by a SEM analysis of the cross section of the wafer surface. In Fig. 2, an example of R is shown in the initial state, after 2 min and after 8 min.

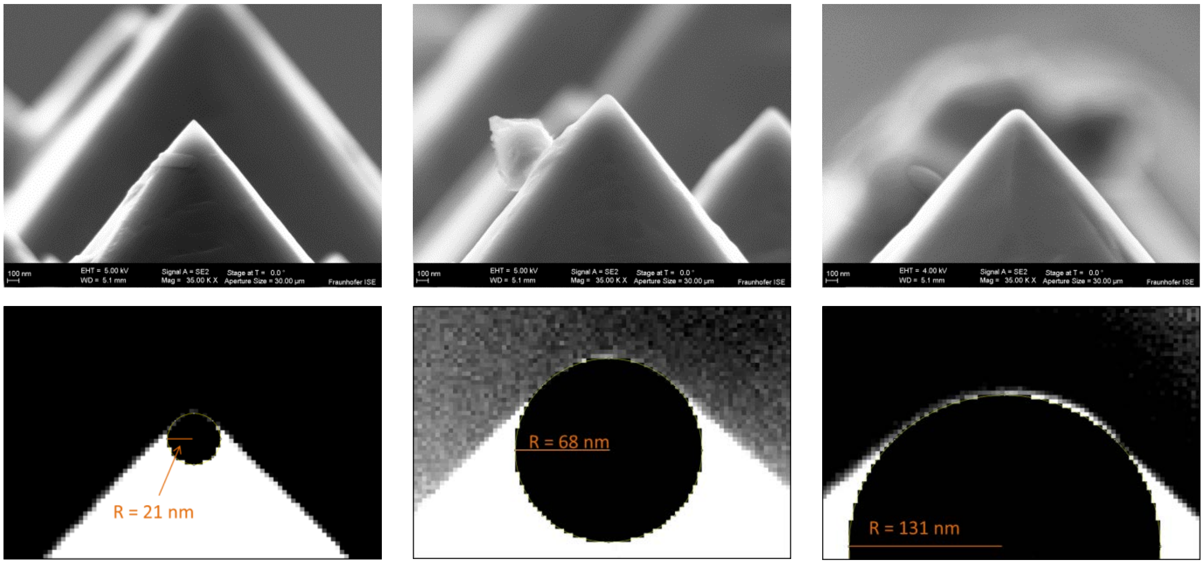

FIGURE 2. SEM analysis of the cross section samples of the micropyramids in the initial state (left), after 2 min (middle) and after 8 min (right) of ozone-based cleaning, with R = 21nm, 68 nm and 131 nm, respectively [5].

Additionally, R was determined for different texture sizes after 0, 2, 4 and 8 minute exposure times (t) (table 1). Texture sizes in this case represent ranges of values for the heights of pyramids present on a wafer surface.

TABLE 1. Experimental data of R of different texturing sizes after exposure time t.

t [min]	**Texture size[μm]**					
	1 - 3		**3 - 5**		**5 - 7**	
	***R* [nm]**	**σ [nm]**	***R* [nm]**	**σ [nm]**	***R* [nm]**	**σ [nm]**
0	18	6	19	6	20	6
2	60	2	67	5	66	4
4	82	0	90	7	79	0
8	131	1	139	18	131	18

The rounding radius and its evolution were almost independent of the texture size. In addition, the initial radius of curvature before cleaning starts was always approximately 20 nm regardless of the texture size. Both the rounding radius and etch rate results were taken as a reference for the design of the simulation model. A mesh convergence study was done to observe the trade-off between simulation accuracy and computational time. The velocity rate constant *k* and the diffusion coefficient *D* of the ozone-based-cleaning were unknown. In order to approach these variables realistically in the simulation model, the parameters were varied and compared with the two data R_{etch} and R obtained from experiments.

2D MODEL

Since O_3 has the largest influence on the etching rate, it is used as the relevant reaction component. With the *Laminar Flow* and *Transport of Diluted Species* interfaces of COMSOL Multiphysics, the diffusion and convection based mass transport of O_3 along the pyramids was described. The flow field was obtained by using the Stokes equation along with the continuity equation. This flow field was used to calculate the convective diffusion in order to find the concentration distribution of O_3 along the pyramid surfaces. In [3] it was shown that the O_3 concentration has an approximately linear influence on the etching rate, so that a first order reaction (1) was assumed. Eq. 4 shows the first order chemical reaction at the moving boundary with c as the position-dependent O_3 concentration in the model, *k* is the etching surface reaction rate constant and **n** is the unit normal vector pointing out towards the computational domain [13].

$$D\nabla c \cdot \mathbf{n} = -kc \tag{4}$$

The deformation v_n of the wafer surface is a function of the reaction rate (4) [13],

$$v_n = \frac{\mathrm{M_{Si}}}{\mathrm{m}\ \rho_{\mathrm{Si}}} \cdot kc \tag{5}$$

with M_{Si} and ρ_{Si} as the molar mass and density of silicon, and m as the stoichiometric factor of the reaction. With the *Deformed Geometry* interface, the deformation of the mesh, and therefore the etch removal was simulated. This interface uses smoothing and mathematical methods to displace the mesh elements of a surface according to a predefined function [14]. A domain with a width of 0.025mm and three pyramids were simulated, Fig. 3.

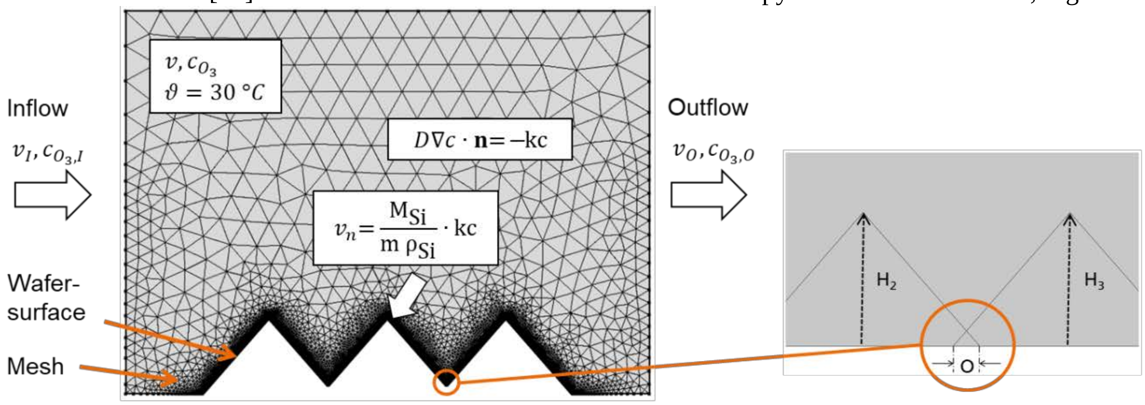

FIGURE 3. Two dimensional simulation model (left), and overlapping O of the pyramids.

The pyramid tips were rounded to R = 20nm since these were the radii of the pyramids in the experiment initial state. The heights of the three pyramids H_1, H_2 H_3 can be selected separately. Due to the *Deformed Geometry* Interface, the pyramids were arranged so that they overlap slightly. For this purpose the overlap O is introduced, Fig. 3 (right). The overlap of the pyramids led to a constant contact of the micro pyramids during simulation despite the shift of the mesh. Otherwise, the deformation process would create a gap between the pyramids that is not defined by the *Deformed Geometry* Interface causing problems in convergence. The evaluation of R_{etch} and R was done on the middle pyramid H_2. The rate constant *k* and diffusion coefficient *D* must be set prior to the variation of the process and geometry parameters. For this purpose, the etching removal over time and the rounding radius R was observed with varying *k* and D. For each parameter variation, a default value is set (table 2). The corresponding parameters with variation values are also given in table 2. While one parameter is varied, the other parameters assumed the default values. In literature, the diffusion coefficient for liquids is in the range of 10^{-9} and 10^{-10} m^2/s [15]. After setting the parameter *D* and *k*, the variation numbers 5 to 6 according to table 2 were carried out. For variation 5 all three pyramids had the same heights of 1 to 7 µm. During variation 5, the effect of different pyramid heights were investigated. Therefore, all combinations of H_1 to H_3 in the range of 3 -5 µm were built and evaluated.

TABLE 2. Default state and variation range of the simulation model at ϑ = 30°C and O = 1µm.

Variation No.	Parameter	Default state	Variation range	Unit
1	D		10^{-9}-10^{-10}	m^2/s
2	k		10-0.01	m/s
3	$c_{O_3,0}$	30	15; 30; 40	mg/l
4	$\dot{V}$	40	20; 40; 60	l/min
5	H_1, H_2, H_3	5	1,1,1 -7,7,7	µm
6	H_1, H_2, H_3		3-5	µm

RESULTS AND DISCUSSION

The first variation results and the etch rate with variation of *D* and *k* are shown in table 3. Since no change in the etching rate with decreasing *k* was found, the finer adjustment of *D* was carried out with k = 1 m/s. With $D = 3.0 \cdot 10^{-10}$ an etching rate of 9.1 nm/min was found, which is in good agreement to the experimental results of approx. 9 nm/min.

TABLE 3. R_{etch} in dependence of k and D.

$D \cdot 10^{-10}$ [m²/s]	0.1	5	10	2.5	3	3.5
***k* [m/s]**			**R_{etch} [nm/min]**			
100	23	14	4.6			
10	23	14	4.6			
1	23	14	4.6	8,0	**9.1**	10.1
0.1	23	14	4.6			

Variation number 2 saw the effect on R by changing k, the results are listed in table 4. No convergence was observed for k = 100 m/s. With decreasing k,, no more isotropic etching prevails, the pyramids become sharper and R no longer agrees with the experimental results. With k = 1 m/s the results are in good agreement with the experimental results (table 5). An image of 3 pyramids after 0, 2, and 8 min exposure time is shown in Fig. 4.

TABLE 4. R in dependence of k with $D = 3.0 \cdot 10^{-10}$ m²/s.

t [min]	Experiment	k = 10	k = 1	k = 0.1	k = 0.01
	R [nm]				
0	19	20	23	20	19
2	67	53	66	50	20
4	90	90	99	86	33
8	139	165	136	153	75

TABLE 5. R_{etch} in dependence of the ozone start concentration $c_{O3,0}$.

$c_{O3,0}$ [mg/l]	Experiment	Simulation
	R_{etch} [nm/min]	
15	≈ 5	5.1
30	≈ 9	9.1
40	≈ 11	12.8

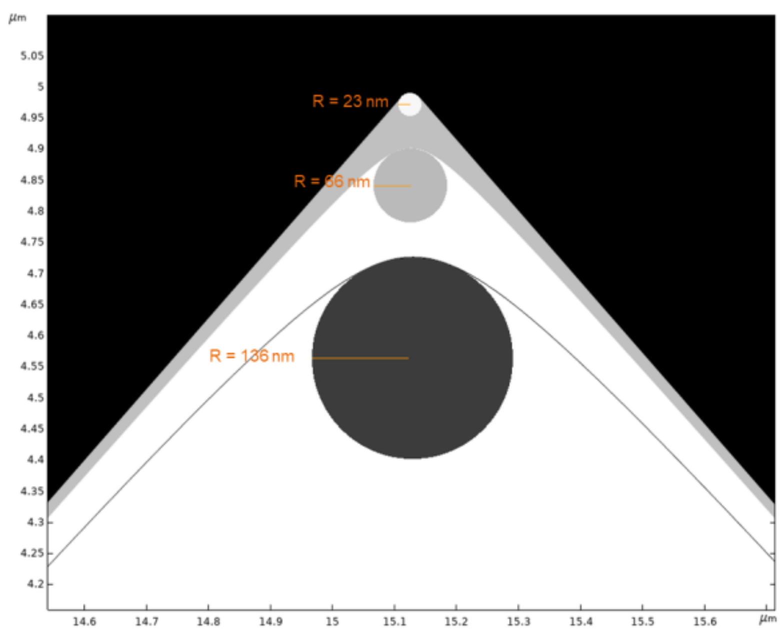

FIGURE 4. Simulation results of the micro pyramids in the initial state, after 2 min and 8 min of ozone-based cleaning, with R = 23nm, 66 nm and 136 nm, with k = 1 m/s and $D = 3.0 \cdot 10^{-10}$ m²/s at $c_{O3,0}$ = 30 mg/l and $\dot{V}$ = 40 l/min, at $H_{1,2,3}$ = 5 µm.

With the set parameter k = 1 m/s and $D = 3.0 \cdot 10^{-10}$ m²/s the next variations were done. In variation number 3 and 4, the R_{etch} dependence of $c_{O3,0}$ and $\dot{V}$ was investigated. In variation number 5 and 6, the impact of different pyramid heights on R_{etch} were investigated. The simulated etch rate for different ozone start concentrations is in good agreement with experimental results (table 5). An increase in the volume flow leads to an increase in the etching rate (table 6). However, this course does not appear to be linear, but rather reaches a saturation state in which a further increase in the volume flow has no influence on the rounding of the pyramids. The mean of the radius of the three different volume flows and the relative standard deviation σ is shown in table 7. The increase in the observed range of the volume flow has no influence on the rounding radius, which is almost the same with 5 – 11% relative standard deviation (table 7).

TABLE 6. R_{etch} in dependence of $\dot{V}$.

$\dot{V}$ [l/min]	R_{etch} [nm/min]
20	8.4
40	9.1
60	11.5

TABLE 7. Mean R of the three different $\dot{V}$ (n=3) and σ for t =2, 4, 8 min.

t [min]	Mean R (n=3) [nm]	σ %
0	21	11
2	59	9
8	135	5

Additionally, the assumption that the etch rate is independent of the pyramid height has not been shown in the simulation, Fig. 5.

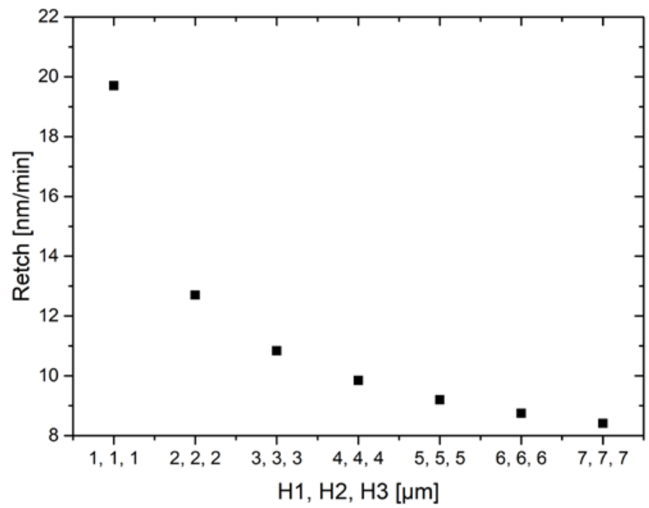

FIGURE 5. R_{etch} for different pyramid heights.

For small pyramids, as the etch rate was almost doubled. Only for larger pyramids did the etch rate appear to reach a limit. The flowmarks that are often observed in ozone baths, assumed from inhomogeneous etching, could appear through areas that have small and large pyramids, which are rounded by the ozone process with different etching rates. Variation number 6, in which H1 to H3 have different heights, shows no significant change in R or R_{etch}. A slight difference can be observed if the middle pyramid is surrounded by two big or small pyramids. Thus, a larger R is seen in the middle pyramids, when it is surrounded by small pyramids and a smaller R when surrounded by large pyramids.

CONCLUSION

An ozone-based simulation model was developed to predict the etch rate (R_{etch}) and rounding radius (R) of micro pyramids without expensive and time-consuming experiments. In the simulation model, the rounding of a pyramid with $k = 1$ m/s and $D = 3{\cdot}10^{-}10$ m^2/s over the exposure time could be observed and is in good agreement to the experimental results. The rounding radii after 2 and 8 min are 67 nm and 139 nm and 66 nm and 136 nm, for the experiment and the simulation, respectively. For the simulation results, the etching rate increases constantly over the O_3 concentration, which is verified with experimental results. The radius also increases with increasing exposure time. With this work, the feasibility of the simulation of the pyramids rounding could be shown. One should note that *k* and *D* were adapted on the basis of the experimental results and were not taken from the literature. Since *D* and *k* are strongly dependent on the temperature, and *k* of ozone varies strongly with pH, in further work these two constants should be investigated more closely. The microscopic 2D-model will be transferred to the macroscopic 3D-model to predict the surface condition of wafers under different influence parameters, e.g. HF, HCl, O_3 concentrations, exposure time, pyramid size, and overlapping of the pyramids, inlet velocity and carrier geometry.

ACKNOWLEDGMENTS

This work was funded by the German Federal Ministry for Economic Affairs and Energy „CHEOPS“ (0324056B).

REFERENCES

1. W. Kern, ed., *Handbook of semiconductor wafer cleaning technology* (Park Ridge, N.J.: Noyes Publications, Park Ridge, N.J, 1993).
2. H. Schröder, Journal of Micromechanics and Microengineering **9** (1999).
3. A. Moldovan, *Ozonbasierte Reinigungs- und Konditionierungsverfahren für die Herstellung hocheffizienter Silizium Solarzellen*. PhD Thesis (Fraunhofer Verlag, Stuttgart, 2016).
4. A. Moldovan, K. Birmann, J. Rentsch, M. Zimmer, T. Gitte, and J. Fittkau, Diffusion and Defect Data Pt.B: Solid State Phenomena **195** (2013).
5. A. Moldovan, A. Fischer, J. Temmler, M. Bivour, T. Dannenberg, D. Erath, A. Lorenz, D. Sontag, J. Zhao, A. Wissen, F. Clement, M. Zimmer, and J. Rentsch, Energy Procedia **124**, 357 (2017).
6. A. Lachowicz, K. Ramspeck, P. Roth, M. Manole, H. Blanke, W. Hefner, E. Brouwer, B. Schum, A. Metz, 27th European Photovoltaic Solar Energy Conference and Exhibition, Frankfurt (2012).
7. A.-K. Volk in *Proceedings*. *CCH Congress Centre and International Fair Hamburg, Germany; Conference 5 - 9 September 2011* (WIP-Renewable Energies), p. 884.
8. I. Kashkoush, G. Chen, D. Nemeth, and J. Rieker, “Wafer surface preparation for high-efficiency solar cells,” in *IEEE 40th Photovoltaic Specialists Conference (PVSC), 2014*. *Colorado Convention Center, Denver, Colorado, 8-13 June 2014* (IEEE, Piscataway, NJ, 2014), p. 1211.
9. S. C. Baker-Finch and K. R. McIntosh, IEEE J. Photovoltaics **1**, 59 (2011).
10. E. J. Bergman, S. Lagrange, M. Claes, S. de Gendt, and E. Röhr, SSP **76-77**, 85 (2001).
11. W. Wibel, *Untersuchungen zu laminarer, transitioneller und turbulenter Strömung in rechteckigen Mikrokanälen*, Zugl.: Dortmund, Techn. Univ., Diss., 2008, Forschungszentrum Karlsruhe, 2009.
12. J. H. Spurk and N. Aksel, *Strömungslehre*. *Einführung in die Theorie der Strömungen ; mit Aufgaben und Übungsbeispielen auf CD-ROM*, 8., überarb. Aufl. (Springer, Berlin, 2010).
13. C. B. Shin and D. J. Economou, J. Electrochem. Soc. **136**, 1997 (1989).
14. COMSOL 5.2a, ed., *COMSOL Multiphysics 5.2*, COMSOL Reference Manual (2016).
15. E. L. Cussler, *Diffusion mass transfer in fluid systems*, 2. ed., 9th printing (Cambridge Univ. Press, Cambridge, 2008).